

Wave Network: An Ultra-Small Language Model

Xin Zhang¹ and Victor S. Sheng²

¹Department of Computer Science, Texas Tech University, 2500 Broadway, Lubbock, Texas, 79409, USA.

²Department of Computer Science, Texas Tech University, 2500 Broadway, Lubbock, Texas, 79409, USA.

Contributing authors: zha19053@ttu.edu; victor.sheng@ttu.edu;

Abstract

We propose an innovative token representation and update method in a new ultra-small language model: the Wave network. Specifically, we use a **complex vector** to represent each token, encoding both global and local semantics of the input text. A **complex vector** consists of two components: a magnitude vector representing the *global semantics* of the input text, and a phase vector capturing the *relationships between individual tokens and global semantics*. Experiments on the AG News text classification task demonstrate that, when generating complex vectors from randomly initialized token embeddings, our single-layer Wave Network achieves 90.91% accuracy with wave interference and 91.66% with wave modulation—outperforming a single Transformer layer using BERT pre-trained embeddings by 19.23% and 19.98%, respectively, and approaching the accuracy of the pre-trained and fine-tuned BERT base model (94.64%). Additionally, compared to BERT base, the Wave Network reduces video memory usage and training time by 77.34% and 85.62% during wave modulation. In summary, we used a 2.4-million-parameter small language model to achieve accuracy comparable to a 100-million-parameter BERT model in text classification.

1 Introduction

Pre-trained token representations are crucial for many language processing models[1], both static token embedding methods, such as Skip-gram and Continuous Bag of Words (CBOW) [2], and context-dependent token embedding methods [3], along with representation updating mechanisms like attention [4], are core techniques in NLP.

Despite the remarkable achievements, current NLP models face several inherent challenges. First, existing token embedding methods primarily focus on local semantics, lacking the ability to directly represent global semantics. Second, popular architectures like Transformer [4] measures semantic similarity using the dot product between token vectors, which is computationally expensive. In multi-layer deep learning architectures, the dot product is computed in each attention head and layer, leading to significant resource demand in terms of computing power and time. Consequently, large language models (LLMs) require numerous layers and substantial hardware, data, and time resources to perform optimally on downstream tasks.

From a more fundamental perspective, Hockett and Hockett [5] suggests that natural language is a complicated signal system that conveys information with specific meanings through the production of sounds and the reception of hearing. The signal characteristics enable human language to express a wide range of abstract concepts. Based on this signal processing view, we focus on an ultra-small language model can approach or even surpass the performance of large language models on specific tasks.

2 Related Work

This research is closely related to multiple fields, including machine learning, natural language processing, and representation learning, which all rely on semantic processing. These fields include applications such as semantic search, knowledge graph, question answering, and various natural language processing techniques. Due to space limitations, we will focus on specific related research areas. For example, Simhi and Markovitch [6] proposed a method to convert a token embedding space into a more understandable concept space, thereby reducing training costs and improving interpretability. Tennenholtz et al. [7] proposed ELM (Embedding Language Model), which makes embeddings more interpretable and broadly applicable by injecting embeddings into LLMs, and then directly transform embedding vectors into understandable narratives. Sun et al. [8] treats the hidden state in RNN (Recurrent Neural Network) [9] as a dynamic, trainable machine learning model,

and this model-based hidden state is updated during the training and testing phases through self-supervised learning rules.

In the Transformer architecture, representation update are carried out through the attention mechanism. Therefore, in addition to research on token embeddings, significant efforts have also been made to improve the attention mechanism itself. For instance, Tay et al. [10] proposed a new and efficient sparse attention learning method based on the differentiable ranking of internal representations. Ding et al. [11] proposed a block-level computation based on local attention to enhance the embedding method of context information. Jaegle et al. [12] proposed the Perceiver, which leverages an asymmetric attention mechanism to iteratively distill inputs into a tight latent bottleneck, allowing it to scale to handle substantial inputs.

3 Method

There are two main token embedding methods. The first one is fixed token embedding, represented by CBOV and Skip-gram, which cannot adapt to the dynamic meanings of tokens in varying contexts. The second is context-dependent embeddings, such as BERT, which generates different embeddings for the same token depending on its contexts. Because most current NLP methods, including Transformer, rely on dot products to measure local semantic similarity between token embeddings, they do not directly capture the global semantics of the entire input text.

In contrast, our framework encodes both global and local semantics using complex vectors. Instead of relying on dot products for token representation updates, we apply addition or multiplication to complex vectors to simulate wave interference or modulation. This approach is possible because languages can be treated as complicated signal systems that convey meaning through sounds production and auditory reception [13, 14], and complex vectors correspond to physical wave representations [15, 16].

3.1 Represent Tokens Using Complex Vectors

We use a **complex vector** $\mathbf{G} \cdot e^{i\alpha}$ to represent each token, encoding both global and local semantics of the input text. A **complex vector** consists of two components: a magnitude vector \mathbf{G} representing the *global semantics* of the input text, and a phase vector α capturing the *relationships between individual tokens and global semantics*. This representation is referred to as **complex vector token representation**. The detailed computation of each component will be explained in the following subsections.

3.1.1 Global Semantics Representation

The meaning of each token in the input text often depends on the overall semantics of the input text. Understanding global semantics helps resolve the ambiguity of individual tokens, which is essential for many downstream tasks requiring a holistic view of the input text.

From a signal processing perspective, *signals are often represented in polar coordinates and processed in the frequency domain*. A signal’s amplitude represents its strength, and its phase describes its position relative to another signal within a cycle [17]. Referring to signal processing, we treat token embeddings as discrete signals in the frequency domain. Given an input text with n tokens $input_text = [\mathbf{w}_1, \mathbf{w}_2, \dots, \mathbf{w}_j, \dots, \mathbf{w}_n]$:

$$\begin{array}{ccc}
 \begin{array}{c}
 \text{dimension 1} \quad \text{dimension } k \\
 \downarrow \qquad \qquad \downarrow \\
 \mathbf{w}_1 = [w_{1,1}, w_{1,2}, \dots, w_{1,k}, \dots, w_{1,768}] \\
 \mathbf{w}_2 = [w_{2,1}, w_{2,2}, \dots, w_{2,k}, \dots, w_{2,768}] \\
 \vdots \qquad \qquad \qquad \vdots \qquad \qquad \qquad \vdots \\
 \mathbf{w}_j = [w_{j,1}, w_{j,2}, \dots, w_{j,k}, \dots, w_{j,768}] \\
 \vdots \qquad \qquad \qquad \vdots \qquad \qquad \qquad \vdots \\
 \mathbf{w}_n = [w_{n,1}, w_{n,2}, \dots, w_{n,k}, \dots, w_{n,768}] \\
 \text{Token Embedding Matrix}
 \end{array}
 &
 &
 \begin{array}{c}
 \text{dimension 1} \quad \text{dimension } k \\
 \downarrow \qquad \qquad \downarrow \\
 [G_{1,1}, G_{1,2}, \dots, G_{1,k}, \dots, G_{1,768}] \\
 [G_{2,1}, G_{2,2}, \dots, G_{2,k}, \dots, G_{2,768}] \\
 \vdots \qquad \qquad \qquad \vdots \qquad \qquad \qquad \vdots \\
 [G_{j,1}, G_{j,2}, \dots, G_{j,k}, \dots, G_{j,768}] \\
 \vdots \qquad \qquad \qquad \vdots \qquad \qquad \qquad \vdots \\
 [G_{n,1}, G_{n,2}, \dots, G_{n,k}, \dots, G_{n,768}] \\
 \text{Token Magnitude Matrix}
 \end{array}
 \end{array} \tag{1}$$

Fig. 1: Token Embedding Matrix and Magnitude Matrix

Note: The number of dimensions can vary. In this proposal, we follow BERT base and use 768 dimensions to facilitate understanding.

Each token embedding \mathbf{w}_j can be treated as a discrete real-value signal, where each elements $w_{j,k}$ represents the signal component along the k -th dimension. From a physical perspective, the magnitude of each signal component is defined as $G_{j,k} = |w_{j,k}|$, and the energy of each signal component can be defined as $E = w_{j,k}^2$ [18]. Using these magnitudes, we calculate the token magnitude matrix (i.e., the right sub-figure in Figure 1) from the token embedding matrix (i.e., the left sub-figure of Figure 1).

Next, we sum the magnitudes of all token embedding components along each dimension to define the **global semantics vector** $\mathbf{G} = [G_1, G_2, \dots, G_k, \dots, G_{768}]$, where each **global semantic element** G_k can be defined as $G_k = \|\mathbf{w}_{:,k}\|_2 = \|[w_{1,k}, w_{2,k}, \dots, w_{j,k}, \dots, w_{n,k}]\|_2 = \sqrt{w_{1,k}^2 + w_{2,k}^2 + \dots + w_{j,k}^2 + \dots + w_{n,k}^2}$, as shown in Figure 2. Here, $w_{j,k}$ represents the k -th dimension of the j -th token embedding. This **global semantic vector** \mathbf{G} represents the global semantics of the entire input text and will serve as the magnitude of the **complex vector token representation** of each token in polar coordinates.

For simplicity, we focus on input-level global semantics in this research. As shown in Figure 1, given a input text with n token embeddings, the input-level global semantics vector can

$$\begin{array}{c}
\text{G} \\
\text{-----} \\
\text{G}_1, \quad \text{G}_2, \quad \dots, \quad \text{G}_k, \quad \dots, \quad \text{G}_{768} \\
\mathbf{w}_1 = \begin{array}{c} \sqrt{w_{1,1}^2} \quad \sqrt{w_{1,2}^2} \dots \sqrt{w_{1,k}^2} \dots \sqrt{w_{1,768}^2} \\ + \\ \sqrt{w_{2,1}^2} \quad \sqrt{w_{2,2}^2} \dots \sqrt{w_{2,k}^2} \dots \sqrt{w_{2,768}^2} \\ + \\ \vdots \\ + \\ \sqrt{w_{j,1}^2} \quad \sqrt{w_{j,2}^2} \dots \sqrt{w_{j,k}^2} \dots \sqrt{w_{j,768}^2} \\ + \\ \vdots \\ + \\ \sqrt{w_{n,1}^2} \quad \sqrt{w_{n,2}^2} \dots \sqrt{w_{n,k}^2} \dots \sqrt{w_{n,768}^2} \end{array}
\end{array}$$

Fig. 2: Global Semantic Vector

be defined as $\mathbf{input_G} = [input_G_1, input_G_2, \dots, input_G_k, \dots, input_G_{768}]$, where $input_G_k = \sqrt{w_{1,k}^2 + w_{2,k}^2 + \dots + w_{j,k}^2 + \dots + w_{n,k}^2}$.

3.1.2 Local Semantics Representation

Local semantics usually represent the specific meaning of individual tokens, which helps in analyzing dependencies and subtle differences between tokens in an input text. For example, tasks like sentiment analysis, entity recognition, and keyword extraction, often require a precise understanding of individual tokens.

1) Using phase to represent relationships between tokens and the global semantic vector

From a signal processing perspective, *phase describes the relative relationships between signals*. We will use the phase of **complex vector token representations** to represent the relative relationships between individual tokens and the **global semantic vector**. That is, the phase representation of a token is coupled with its **global semantic vector**. For each token w_j in the input text, its **phase vector** is $\alpha_j = [\alpha_1, \alpha_2, \dots, \alpha_k, \dots, \alpha_{768}] = [input_alpha_1, input_alpha_2, \dots, input_alpha_k, \dots, input_alpha_{768}]$, where $input_alpha_k$ is defined as $arctan2(\frac{\sqrt{1 - (\frac{w_{j,k}}{input_G_k})^2}}{\frac{w_{j,k}}{input_G_k}})$ based on the corresponding element $input_G_k$ in the **global semantic vector** of the input text $\mathbf{input_G} = [input_G_1, input_G_2, \dots, input_G_k, \dots, input_G_{768}]$. Note that we use the function $arctan2$ to ensure angles fall within the range of $-\pi$ to π , consistent with the standard phase angle in physics. With these definitions, we can derive the token phase matrix (i.e., the right sub-figure in Figure 3) from the token embedding matrix (the left sub-figure of Figure 3).

$$\begin{array}{cc}
\mathbf{w}_1 = [w_{1,1}, w_{1,2}, \dots, w_{1,k}, \dots, w_{1,768}] & \alpha_1 = [\alpha_{1,1}, \alpha_{1,2}, \dots, \alpha_{1,k}, \dots, \alpha_{1,768}] \\
\mathbf{w}_2 = [w_{2,1}, w_{2,2}, \dots, w_{2,k}, \dots, w_{2,768}] & \alpha_2 = [\alpha_{2,1}, \alpha_{2,2}, \dots, \alpha_{2,k}, \dots, \alpha_{2,768}] \\
\vdots & \vdots \\
\mathbf{w}_j = [w_{j,1}, w_{j,2}, \dots, w_{j,k}, \dots, w_{j,768}] & \alpha_j = [\alpha_{j,1}, \alpha_{j,2}, \dots, \alpha_{j,k}, \dots, \alpha_{j,768}] \\
\vdots & \vdots \\
\mathbf{w}_n = [w_{n,1}, w_{n,2}, \dots, w_{n,k}, \dots, w_{n,768}] & \alpha_n = [\alpha_{n,1}, \alpha_{n,2}, \dots, \alpha_{n,k}, \dots, \alpha_{n,768}]
\end{array} \tag{2}$$

Token Embedding Matrix
Token Phase Matrix

Fig. 3: Token Embedding Matrix and Phase Matrix

2) Illustrate Complex Vector Token Representation in Cartesian coordinate system

To illustrate the meaning of **complex vector token representations**' components in Cartesian coordinates, we use the Euler's formula $e^{i\theta} = \cos(\theta) + i \cdot \sin(\theta)$ [19] to convert **complex vector token representations** from polar to Cartesian coordinates, as shown in Figure 4. For example, the **complex vector token representations** $\mathbf{input_G}$ can be expressed in Cartesian coordinates as $\mathbf{input_G} \cdot \cos(\mathbf{input_alpha}_j) + i \cdot \mathbf{input_G} \cdot \sin(\mathbf{input_alpha}_j)$. The inner product of $\sin(\mathbf{input_alpha}_j)$ and $\cos(\mathbf{input_alpha}_j)$ is zero over a full period, making them orthogonal [20]. Consequently, the real part $\mathbf{input_G} \cdot \cos(\mathbf{input_alpha}_j)$ and the imaginary part $i \cdot \mathbf{input_G} \cdot \sin(\mathbf{input_alpha}_j)$ are also orthogonal, fulfilling the properties of wave representations as described in physics [21]. As Figure 4 illustrates, the real part of the token embedding w_j represents the token's contribution along the k -th dimension, capturing the local semantics of the input text. The imaginary part describes the **global semantic element** apart from w_j , representing the context of token w_j along the k -th dimension within the input text.

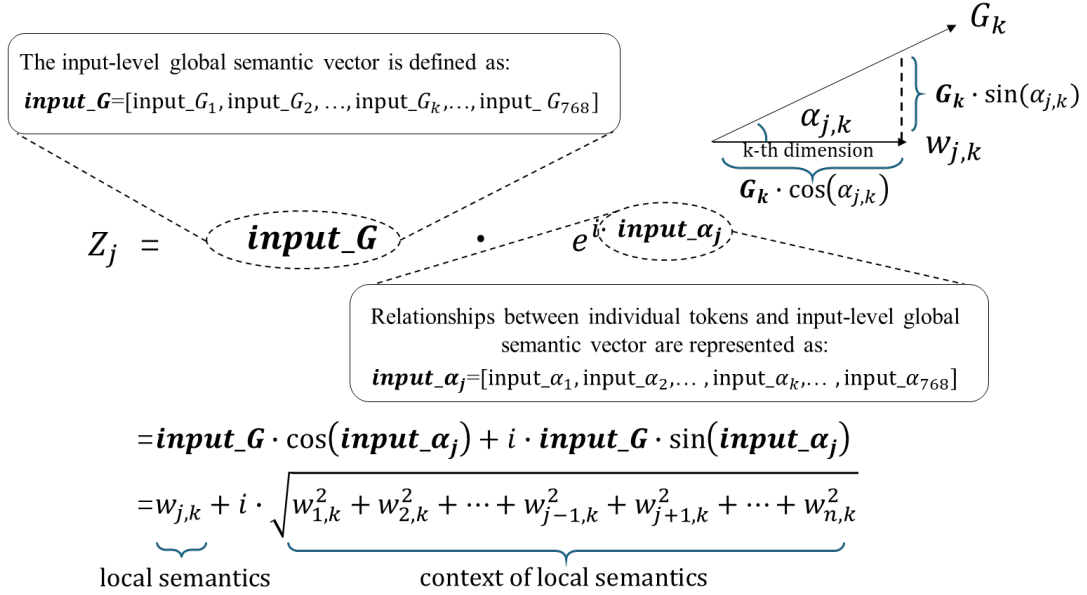


Fig. 4: Convert **complex vector token representations** from polar coordinates to Cartesian coordinates

3) An example of a Complex Vector Token Representation

Figure 5 provides an example illustrating how to convert each token in an input text “I am alive” into **complex vector token representations** in four steps: First, we randomly generate embeddings in a 768-dimension feature space for all three tokens in the input text; Second, we calculate the **global semantic vector** of all three token embeddings across all dimensions; Third, we compute the component $\alpha_{j,k}$ of the phase vector α_j for each tokens. And finally, we combine the **global semantic vector** \mathbf{G} and the **phase vector** α_j to compose a **complex vector token representations** for each token w_j in polar coordinates.

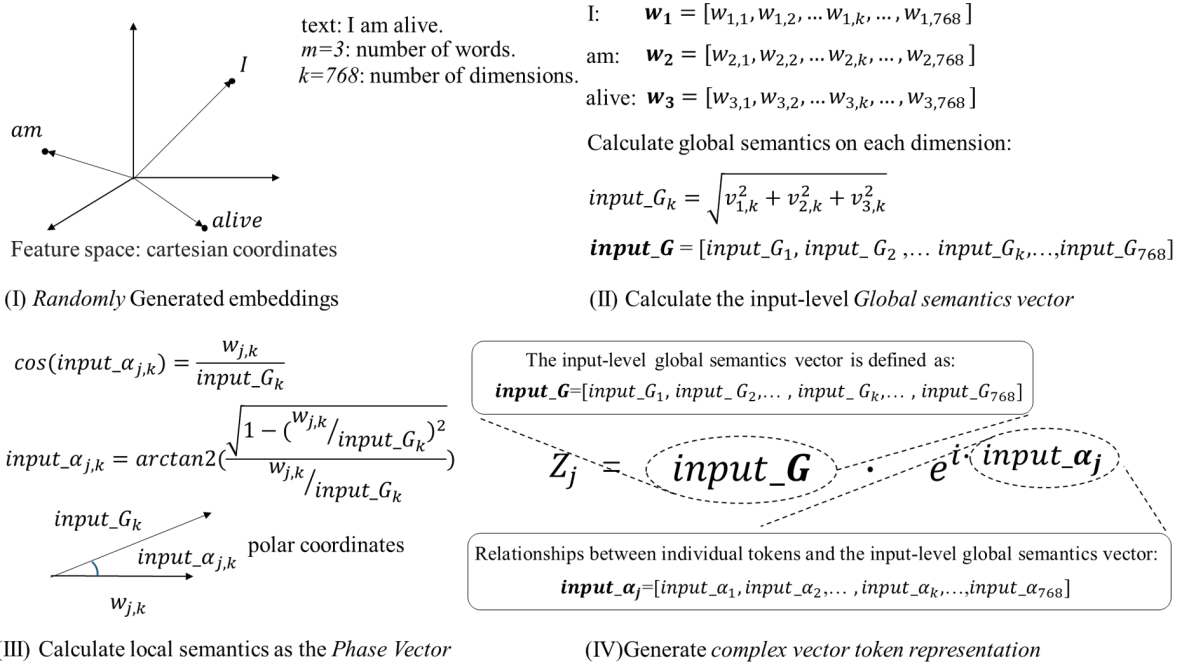


Fig. 5: An example of constructing representations with **complex vector token representations**

3.2 Update Wave Representation by Superposition

Complex vectors correspond to physical wave representations [15, 16], which allows us to use wave-based operations for more efficient **complex vector token representations** updates. We propose to develop a linear layer in our Wave network to generate two variants of the input-text level **complex vector token representation** of each token. These two variants can then be used for applying wave-based operations, such as interference and modulation to model **complex vector token representation** updates more effectively.

3.2.1 Wave Interference

From physical perspective, *wave interference is a phenomenon where two coherent waves combined by adding their intensities or displacements, considering their phase difference*. In the context of generating **complex vector token representations** from input-level global semantics, as discussed in the Subsection 3.1.1, we consider two variants of **complex vector token representations** for token w_j as: $\mathbf{input_Z}_j =$

$\mathbf{input_G} \cdot e^{i \cdot \mathbf{input_}\alpha_j}$ and $\mathbf{input_Z}'_j = \mathbf{input_G}' \cdot e^{i \cdot \mathbf{input_}\alpha'_j}$. We use complex vectors addition to simulate wave interference [22] and obtain the combined **complex vector token representation interference_Zj** for token w_j as follows:

$$\begin{aligned} \mathbf{Interference_Zj} &= \mathbf{input_Zj} + \mathbf{input_Z}'_j = \mathbf{input_G} \cdot e^{i \cdot \mathbf{input_}\alpha_j} + \mathbf{input_G}' \cdot e^{i \cdot \mathbf{input_}\alpha'_j} \\ &= \left(\mathbf{input_G} \cdot \cos(\mathbf{input_}\alpha_j) + \mathbf{input_G}' \cdot \cos(\mathbf{input_}\alpha'_j) \right) \\ &\quad + i \cdot \left(\mathbf{input_G} \cdot \sin(\mathbf{input_}\alpha_j) + \mathbf{input_G}' \cdot \sin(\mathbf{input_}\alpha'_j) \right) \end{aligned} \quad (3)$$

, where the last equation is based on Euler's formula: $e^{i\theta} = \cos(\theta) + i \sin(\theta)$.

Then, based on the definitions of the $\mathbf{input_G}$ and $\mathbf{input_}\alpha_j$ provided in the Subsection 3.1.1 and 3.1.2, the components of Equation 3 can be expressed explicitly for the k -th component of the token w_j 's **complex vector token representation** as:

$$\begin{aligned} \mathbf{Interference_Zj,k} &= \sqrt{w_{1,k}^2 + w_{2,k}^2 + \dots + w_{j,k}^2 + \dots + w_{n,k}^2} \cdot \frac{w_{j,k}}{\sqrt{w_{j,k}^2 + w_{2,k}^2 + \dots + \dots + w_{j,k}^2 + \dots + w_{n,k}^2}} \\ &\quad + \sqrt{w'_{1,k}{}^2 + w'_{2,k}{}^2 + \dots + w'_{j,k}{}^2 + \dots + w'_{n,k}{}^2} \cdot \frac{w'_{j,k}}{\sqrt{w'_{j,k}{}^2 + w'_{2,k}{}^2 + \dots + \dots + w'_{j,k}{}^2 + \dots + w'_{n,k}{}^2}} \\ &\quad + i \cdot \left(\sqrt{w_{1,k}^2 + w_{2,k}^2 + \dots + w_{j,k}^2 + \dots + w_{n,k}^2} \right) \cdot \left(\sqrt{1 - \left(\frac{w_{j,k}}{\sqrt{w_{1,k}^2 + w_{2,k}^2 + \dots + w_{j,k}^2 + \dots + w_{n,k}^2}} \right)^2} \right) \\ &\quad + i \cdot \left(\sqrt{w'_{1,k}{}^2 + w'_{2,k}{}^2 + \dots + w'_{j,k}{}^2 + \dots + w'_{n,k}{}^2} \right) \cdot \left(\sqrt{1 - \left(\frac{w'_{j,k}}{\sqrt{w'_{1,k}{}^2 + w'_{2,k}{}^2 + \dots + w'_{j,k}{}^2 + \dots + w'_{n,k}{}^2}} \right)^2} \right) \\ &= w_{j,k} + w'_{j,k} + i \cdot \left(\sqrt{w_{1,k}^2 + w_{2,k}^2 + \dots + w_{j-1,k}^2 + w_{j+1,k}^2 + \dots + w_{n,k}^2} \right) \\ &\quad + \sqrt{w'_{1,k}{}^2 + w'_{2,k}{}^2 + \dots + w'_{j-1,k}{}^2 + w'_{j+1,k}{}^2 + \dots + w'_{n,k}{}^2} \end{aligned} \quad (4)$$

Next, we will illustrate how the phase difference of two **complex vector token representations**, such as $\mathbf{input_Zj}$ and $\mathbf{input_Z}'_j$, affects the overall intensity of the resulting **complex vector token representation** by analyzing their interference term. As mentioned in [23, 24], the interference term $\text{Re}(\mathbf{input_Zj} \cdot \overline{\mathbf{input_Z}'_j})$ can be obtained from the square of the magnitude of $\mathbf{input_Zj,k} = |\mathbf{input_Zj} + \mathbf{input_Z}'_j|^2 = |\mathbf{input_Zj}|^2 + |\mathbf{input_Z}'_j|^2 + 2 \cdot (\mathbf{input_Zj} \cdot \overline{\mathbf{input_Z}'_j})$, which describes how the phase difference between two **complex vector token representations** determines whether they interfere constructively or destructively. $\overline{\mathbf{input_Zj}}$ is the complex conjugate of $\mathbf{input_Zj}$, which is used to ensure that as a measurable physical quantity, the intensity is a real value [25]. We can further express the interference term as:

$$\begin{aligned} 2 \cdot \text{Re}(\mathbf{input_Zj} \cdot \overline{\mathbf{input_Z}'_j}) &= 2 \cdot \text{Re} \left(\mathbf{input_G} \cdot e^{i \cdot \mathbf{input_}\alpha_j} \cdot \mathbf{input_G}' \cdot e^{-i \cdot \mathbf{input_}\alpha'_j} \right) \\ &= 2 \cdot \mathbf{input_G} \cdot \mathbf{input_G}' \cdot \cos(\mathbf{input_}\alpha_j - \mathbf{input_}\alpha'_j) \end{aligned} \quad (5)$$

Equation 5 demonstrates that the cosine value of the phase difference directly determines the interference result.

3.2.2 Wave Modulation

From a physical perspective, *wave modulation is the process of varying one or more properties of a periodic waveform, called the carrier signal, with a separate signal, which contains the information to be transmitted.* From a signal processing perspective, *adjusting the amplitude of a carrier wave in accordance with the input signal is referred to as amplitude modulation [26]. Similarly, adjusting the phase of a carrier wave in accordance with the input signal is referred to as phase modulation [27].* Both amplitude modulation and phase modulation can be achieved through the multiplication of complex vectors representing waves [28–30].

In the context of generating **complex vector token representations** from input-level global semantics, as discussed in the Subsection 3.1.1, we consider two variants of **complex vector token representations** for token w_j as: $\mathbf{input_Zj} = \mathbf{input_G} \cdot e^{i \cdot \mathbf{input_}\alpha_j}$ and $\mathbf{input_Z}'_j = \mathbf{input_G}' \cdot e^{i \cdot \mathbf{input_}\alpha'_j}$. We use complex vectors multiplication to simulate wave modulation [22] and obtain the combined **complex vector token representation modulation_Zj** for token w_j as follows:

$$\begin{aligned}
\text{Modulation_Z}_j &= \text{input_Z}_j \cdot \text{input_Z}'_j = \text{input_G} \cdot e^{i \cdot \text{input_}\alpha_j} \cdot \text{input_G}' \cdot e^{i \cdot \text{input_}\alpha'_j} \\
&= \text{input_G} \cdot \text{input_G}' \cdot e^{i \cdot \text{input_}\alpha_j + \text{input_}\alpha'_j} \\
&= \text{input_G} \cdot \text{input_G}' \cdot \cos(\text{input_}\alpha_j + \text{input_}\alpha'_j) \\
&\quad + i \cdot \text{input_G} \cdot \text{input_G}' \cdot \sin(\text{input_}\alpha_j + \text{input_}\alpha'_j)
\end{aligned} \tag{6}$$

Here, the amplitude modulation term is represented by $\text{input_G} \cdot \text{input_G}'$. And the phase modulation term is expressed as $\text{input_}\alpha_j + \text{input_}\alpha'_j$. Then, based on the definitions of the input_G and $\text{input_}\alpha_j$ provided in the Subsection 3.1.1 and 3.1.2, the components of Equation 6 can be expressed explicitly for the k -th component of the token w_j 's **complex vector token representation** as:

$$\begin{aligned}
\text{Modulation_Z}_{j,k} &= \sqrt{w_{1,k}^2 + w_{2,k}^2 + \dots + w_{j,k}^2 + \dots + w_{n,k}^2} \cdot \sqrt{w'_{1,k}{}^2 + w'_{2,k}{}^2 + \dots + w'_{j,k}{}^2 + \dots + w'_{n,k}{}^2} \\
&\cdot \left(\frac{w_{j,k}}{\sqrt{w_{1,k}^2 + w_{2,k}^2 + \dots + w_{j,k}^2 + \dots + w_{n,k}^2}} \cdot \frac{w'_{j,k}}{\sqrt{w'_{1,k}{}^2 + w'_{2,k}{}^2 + \dots + w'_{j,k}{}^2 + \dots + w'_{n,k}{}^2}} \right. \\
&\quad \left. - \sqrt{1 - \left(\frac{w_{j,k}}{\sqrt{w_{1,k}^2 + w_{2,k}^2 + \dots + w_{j,k}^2 + \dots + w_{n,k}^2}} \right)^2} \cdot \sqrt{1 - \left(\frac{w'_{j,k}}{\sqrt{w'_{1,k}{}^2 + w'_{2,k}{}^2 + \dots + w'_{j,k}{}^2 + \dots + w'_{n,k}{}^2}} \right)^2} \right) \\
&+ i \cdot \sqrt{w_{1,k}^2 + w_{2,k}^2 + \dots + w_{j,k}^2 + \dots + w_{n,k}^2} \cdot \sqrt{w'_{1,k}{}^2 + w'_{2,k}{}^2 + \dots + w'_{j,k}{}^2 + \dots + w'_{n,k}{}^2} \\
&\cdot \left(\sqrt{1 - \left(\frac{w_{j,k}}{\sqrt{w_{1,k}^2 + w_{2,k}^2 + \dots + w_{j,k}^2 + \dots + w_{n,k}^2}} \right)^2} \cdot \frac{w'_{j,k}}{\sqrt{w'_{1,k}{}^2 + w'_{2,k}{}^2 + \dots + w'_{j,k}{}^2 + \dots + w'_{n,k}{}^2}} \right. \\
&\quad \left. + \frac{w_{j,k}}{\sqrt{w_{1,k}^2 + w_{2,k}^2 + \dots + w_{j,k}^2 + \dots + w_{n,k}^2}} \cdot \sqrt{1 - \left(\frac{w'_{j,k}}{\sqrt{w'_{1,k}{}^2 + w'_{2,k}{}^2 + \dots + w'_{j,k}{}^2 + \dots + w'_{n,k}{}^2}} \right)^2} \right) \\
&= (w_{j,k} \cdot w'_{j,k} - \sqrt{w_{1,k}^2 + w_{2,k}^2 + \dots + w_{j-1,k}^2 + w_{j+1,k}^2 + \dots + w_{n,k}^2} \\
&\quad \cdot \sqrt{w'_{1,k}{}^2 + w'_{2,k}{}^2 + \dots + w'_{j-1,k}{}^2 + w'_{j+1,k}{}^2 + \dots + w'_{n,k}{}^2}) \\
&+ i \cdot (w'_{j,k} \cdot \sqrt{w_{1,k}^2 + w_{2,k}^2 + \dots + w_{j-1,k}^2 + w_{j+1,k}^2 + \dots + w_{n,k}^2} \\
&\quad + (w_{j,k} \cdot \sqrt{w'_{1,k}{}^2 + w'_{2,k}{}^2 + \dots + w'_{j-1,k}{}^2 + w'_{j+1,k}{}^2 + \dots + w'_{n,k}{}^2}))
\end{aligned} \tag{7}$$

4 Single-layer and Multi-layer Architecture of the Wave Network

a) Single layer architecture:

To implement the operations of generating and updating **complex vector token representations**, we designed a deep learning model called the Wave network. Figure 6a illustrates the layer-level design of the Wave network. Starting with an input text, we generate initial embeddings for each token by randomly assigning values across 768 dimensions. These initial embeddings serve as the basis for generating a single **wave representation** representing input-level global semantics, with positional encoding included. Using a linear layer, we create two variants of this **wave representation**, which are then modulated through multiplication. The resulting representation is passed through a feed-forward layer and a normalization layer. Finally, the processed representations are used as the foundation for subsequent classification tasks.

b) Multi-layer architecture:

Figure 6b shows the structure of one block in a multi-layer Wave network, which mathematical expressions can be represented as:

$$\mathbf{W}_{n+1} = \mathbf{W}_n + D(g(f_{n+1}(\mathbf{W}_n))) \tag{8}$$

Where \mathbf{W}_n is the output of the n -th layer, $f_{n+1}(\mathbf{W}_n)$ denotes the wave overlay of the $(n+1)$ -th layer, $g(x)$ convert complex number to token embedding, and $D(x)$ the dropout operation applied to the input x .

5 Experiments and Results

The parameters across all experiments are kept as consistent as possible. The learning rate for both the Wave network and Transformer learning rate is set to 1e-3, while for BERT, it is set to 2e-5[31]. The batch size varies depending on the task. In the resource utilization comparison experiments, all models use a batch size of 64. In the accuracy comparison experiments, the batch size is 64 for the Wave network and Transformer, and 32 for BERT[31]. In the gradient comparison and embedding independence experiments, all three models use a batch size of 32. All models are trained or fine-tuned for four epochs. In the fast convergence experiments, we use 500 batches and record the accuracy on the test set every ten batches. The Wave network and Transformer use a

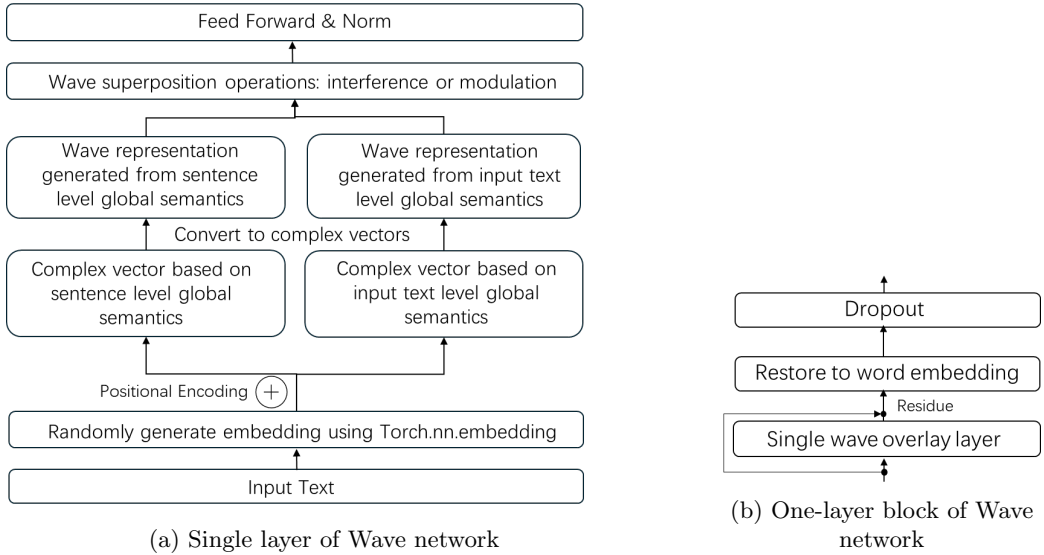


Fig. 6: Single layer and multi-layer design of the Wave Network

single-layer design; the Wave network generates initial token embeddings randomly using torch.nn.embedding in Pytorch[32], while the Transformer uses token embeddings from pre-trained BERT. For BERT experiments, the base pre-trained model is fine-tuned. In Table 7 and 2, VRAM usage is measured in gigabytes(GB), and the time consumed per epoch(for both training and fine-tuning) is measured in seconds. All preliminary experiments are conducted on AG News[33], DBpedia14[34], and IMDB[35] datasets, with an 80/20 training-validation split. Each data has a separated test subset.

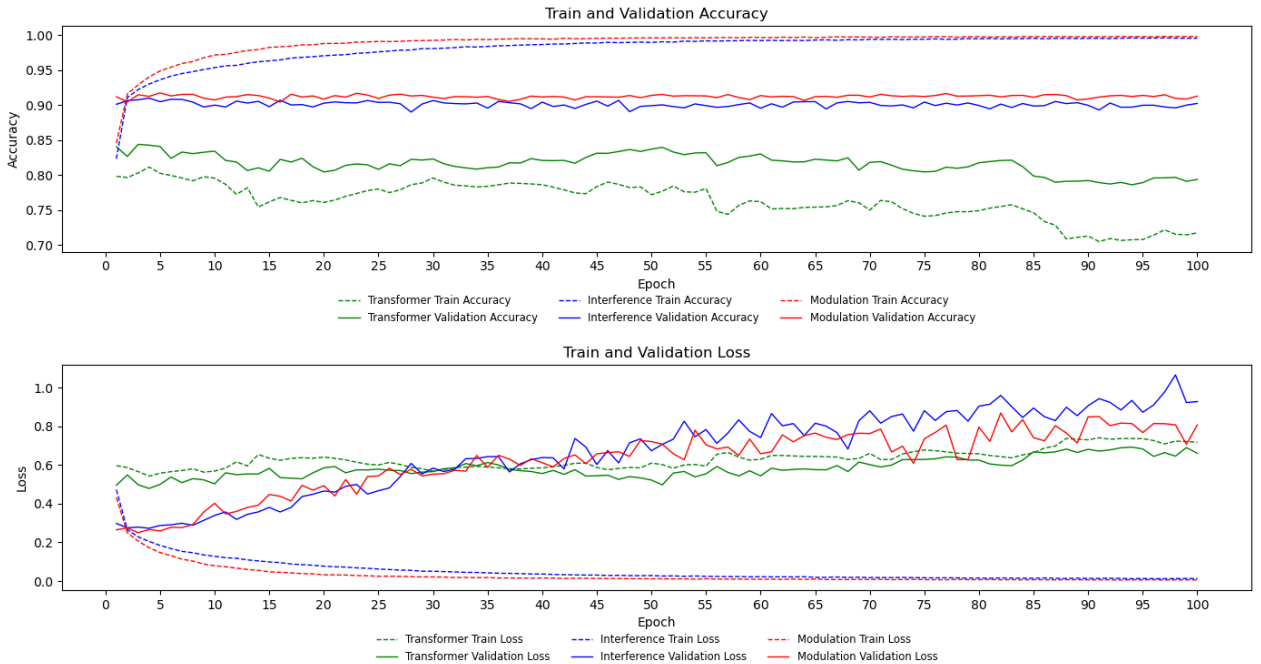


Fig. 7: Comparison between Wave Network and Transformer

Model	Data sets	Accuracy	VRAM(GB)	Time(s)
Wave network (Interference)	AG News	90.36%	0.30	146.90
Wave network (Modulation)	AG News	91.29%	0.32	147.02
Transformer	AG News	71.68%	0.85	173.25

Table 1: Performance Comparison between Wave Network and Transformer on AG News

As shown in Table 1 and Table 2 for the AG News dataset, compared to the single-layer Transformer, a single-layer Wave network achieved 90.36% accuracy with wave interference and 91.29% with wave modulation,

Model	Data sets	Accuracy	VRAM(GB)	Time(s)
Wave network (Interference)	AG News	90.91%	0.30	146.90
Wave network (Modulation)	AG News	91.66%	0.32	147.02
BERT base	AG News	94.64%	1.28	1034.99
Wave network (Interference)	DBpedia14	97.93%	0.30	979.78
Wave network (Modulation)	DBpedia14	98.05%	0.30	991.15
BERT base	DBpedia14	99.28%	1.27	2734.76
Wave network (Interference)	IMDB	87.00%	0.37	119.57
Wave network (Modulation)	IMDB	87.02%	0.37	119.96
BERT base	IMDB	93.94%	1.27	220.46

Table 2: Performance Comparison between Wave Network and BERT on Various Data Sets

outperforming a single Transformer layer by 18.68% and 19.61%, respectively, and approaching the BERT base model’s 94.64%. At the same time, the Wave network reduced video memory usage and training time by 77.34% and 85.62% during wave modulation compared to BERT base.

6 Discussion

The Wave Network introduces an efficient token representation method that uses complex vectors to encode global and local text semantics, allowing it to perform competitively on NLP tasks with significantly reduced computational demands. By simulating wave interference and modulation, the model achieves high accuracy with much lower VRAM usage and training time compared to larger models like BERT base. This efficiency not only highlights its potential for resource-limited devices but also paves the way for scalable NLP applications that can be deployed in real-time environments, from mobile devices to embedded systems without sacrificing performance.

References

- [1] Peters, M.E., Neumann, M., Iyyer, M., Gardner, M., Clark, C., Lee, K., Zettlemoyer, L.: Deep contextualized word representations. arXiv preprint [abs/1802.05365](https://arxiv.org/abs/1802.05365)(cs.CL), 1–27 (2018)
- [2] Mikolov, T.: Efficient estimation of word representations in vector space. arXiv preprint arXiv [1301](https://arxiv.org/abs/1301.3781)(3781) (2013)
- [3] Devlin, J., Chang, M.-W., Lee, K., Toutanova, K.: Bert: Pre-training of deep bidirectional transformers for language understanding. arXiv preprint [arXiv:1810.04805](https://arxiv.org/abs/1810.04805) (2019)
- [4] Vaswani, A., Shazeer, N., Parmar, N., Uszkoreit, J., Jones, L., Gomez, A.N., Kaiser, L., Polosukhin, I.: Attention is all you need. arXiv preprint arXiv:1706.03762 [abs/1706.03762](https://arxiv.org/abs/1706.03762)(1), 1–15 (2023)
- [5] Hockett, C.F., Hockett, C.D.: The origin of speech. *Scientific American* **203**(3), 88–97 (1960)
- [6] Simhi, A., Markovitch, S.: Interpreting embedding spaces by conceptualization. arXiv preprint [2209](https://arxiv.org/abs/2209.00445)(00445) (2022)
- [7] Tennenholtz, G., Chow, Y., Hsu, C.-W., Jeong, J., Shani, L., Tulepbergenov, A., Ramachandran, D., Mladenov, M., Boutilier, C.: Demystifying embedding spaces using large language models. arXiv preprint [2310](https://arxiv.org/abs/2310.04475)(04475) (2023)
- [8] Sun, Y., Li, X., Dalal, K., Xu, J., Vikram, A., Zhang, G., Dubois, Y., Chen, X., Wang, X., Koyejo, S., et al.: Learning to (learn at test time): Rnns with expressive hidden states. arXiv preprint [2407](https://arxiv.org/abs/2407.04620)(04620) (2024)
- [9] Rumelhart, D.E., Hinton, G.E., Williams, R.J.: Learning representations by back-propagating errors. *Nature* **323**(6088), 533–536 (1986)
- [10] Tay, Y., Bahri, D., Yang, L., Metzler, D., Juan, D.-C.: Sparse sinkhorn attention. In: International Conference on Machine Learning, vol. 119, pp. 9438–9447. PMLR, ??? (2020)
- [11] Ding, L., Tang, H., Bruzzone, L.: Lanet: Local attention embedding to improve the semantic segmentation of remote sensing images. *IEEE Transactions on Geoscience and Remote Sensing* **59**(1), 426–435 (2020)
- [12] Jaegle, A., Gimeno, F., Brock, A., Vinyals, O., Zisserman, A., Carreira, J.: Perceiver: General perception with iterative attention. In: International Conference on Machine Learning, vol. 139, pp. 4651–4664. PMLR, ??? (2021)
- [13] Fleisch, D., Kinnaman, L.: A student’s guide to waves (2019)

- [14] Towne, D.H.: Wave Phenomena. Courier Dover Publications, ??? (2014)
- [15] Berman, P.R., Coughlin: Introductory Quantum Mechanics. Springer, ??? (2018)
- [16] Herman, R.L.: Introduction to partial differential equations. North Carolina, NC, USA: RL Herman (2015)
- [17] Feynman, R.P., Leighton, R.B., Sands, M.: The Feynman Lectures on Physics; New Millennium Ed. Basic Books, New York, NY (2010). Originally published 1963-1965. <https://cds.cern.ch/record/1494701>
- [18] Oppenheim, A.V., Willsky, A.S., Nawab, S.H.: Signals & Systems (2nd Ed.). Prentice-Hall, Inc., USA (1996)
- [19] Ahlfors, L.V.: Complex Analysis, 2nd edn. McGraw-Hill Book Company
- [20] Arfken, G.B., Arfken, G.B., Weber, H.J., Harris, F.E.: Mathematical Methods for Physicists: A Comprehensive Guide. Elsevier Science, ??? (2013). https://books.google.com/books?id=qLFo_Z-PoGIC
- [21] Jackson, J.D.: Classical Electrodynamics, 3rd ed. edn. Wiley, New York, NY (1999). <http://cdsweb.cern.ch/record/490457>
- [22] OpenStax: University Physics Volume 1. OpenStax, ??? (2024). <https://openstax.org/books/university-physics-volume-1/pages/16-5-interference-of-waves>
- [23] Born, M., Wolf, E., Bhatia, A.B.: Principles of Optics. Cambridge University Press, ??? (2019). <https://books.google.com/books?id=FsS-DwAAQBAJ>
- [24] Hecht, E.: Optics, 5th edn. Pearson, ??? (2016)
- [25] Griffiths, D.J.: Introduction to Electrodynamics, 4th edn. Cambridge University Press, ??? (2017)
- [26] Georgi, H.: The Physics of Waves. Prentice Hall, ??? (1993). <https://books.google.com/books?id=gajvAAAAMAAJ>
- [27] Taub, H., Schilling, D.L.: Principles of Communication Systems, 2nd edn. McGraw-Hill Higher Education, ??? (1986)
- [28] Crecraft, D.I., Gergely, S.: 9 - radio communication techniques. In: Crecraft, D.I., Gergely, S. (eds.) Analog Electronics, pp. 200–232. Butterworth-Heinemann, Oxford (2002). <https://doi.org/10.1016/B978-075065095-3/50009-X> . <https://www.sciencedirect.com/science/article/pii/B978075065095350009X>
- [29] Pursley, M.B.: 23 - analog communications. In: Middleton, W.M., Van Valkenburg, M.E. (eds.) Reference Data for Engineers (Ninth Edition), Ninth edition edn., pp. 23–12319. Newnes, Woburn (2002). <https://doi.org/10.1016/B978-075067291-7/50025-X> . <https://www.sciencedirect.com/science/article/pii/B978075067291750025X>
- [30] James, G.: Digital phase modulation: A review of basic concepts. Chief Scientist Transcript International, Inc (2003)
- [31] Sun, C., Qiu, X., Xu, Y., Huang, X.: How to fine-tune bert for text classification? In: Chinese Computational Linguistics: 18th China National Conference, CCL 2019, Kunming, China, October 18–20, 2019, Proceedings 18, pp. 194–206 (2019). Springer
- [32] Paszke, A., Gross, S., Massa, F., Lerer, A., Bradbury, J., Chanan, G., Killeen, T., Lin, Z., Gimelshein, N., Antiga, L., et al.: Pytorch: An imperative style, high-performance deep learning library. Advances in neural information processing systems **32** (2019)
- [33] Zhang, X., Zhao, J., LeCun, Y.: Character-level convolutional networks for text classification. Advances in Neural Information Processing Systems **28** (2015)
- [34] Auer, S., Bizer, C., Kobilarov, G., Lehmann, J., Cyganiak, R., Ives, Z.: Dbpedia: A nucleus for a web of open data. In: International Semantic Web Conference, pp. 722–735 (2007). Springer
- [35] Maas, A., Daly, R.E., Pham, P.T., Huang, D., Ng, A.Y., Potts, C.: Learning word vectors for sentiment analysis. In: Proceedings of the 49th Annual Meeting of the Association for Computational Linguistics: Human Language Technologies, pp. 142–150 (2011)